International Journal of Minerals, Metallurgy and Materials
Accepted manuscript, https://doi.org/10.1007/s12613-020-2150-9

Electrochemical properties of Ca-Pb electrode for calcium-based liquid metal batteries

Xiao-hui Ning, Chen-zheng Liao, Guo-qing Li*

Center for Advancing Materials Performance from the Nanoscale (CAMP-Nano), State Key Laboratory for Mechanical Behavior of Materials, Xi'an Jiaotong University, Xi'an 710049, China

*Coresponding author: xiaohuining@mail.xjtu.edu.cn

Abstract

The Ca-Pb electrode couple was considered to be one of the lowest cost (~36 $ kWh^{-1}) among various optional materials for liquid metal battery. The electrochemical properties of Ca-Pb alloy in the Ca|LiCl-NaCl-$CaCl_2$|Pb cell were investigated in this paper. The electrode potential maintains a linear relationship in the current density range from 50 to 200 mA cm^{-2}, which indicates that the alloying and dealloying process of Ca with Pb have the rapid charge transfer and mass transport in the interface between the liquid electrode and liquid electrolyte. The Ca-Pb electrode exhibits great properties with a high discharge voltage of 0.6 V, a small self-discharge current density (< 2 mA cm^{-2} at 600°C) and a high coulombic efficiency (> 99%). The post-mortem analysis shows that the intermetallics $CaPb_3$ and CaPb were uniformly distributed in the electrode, which indicates that the nucleation of solid intermetallics will not hinder the diffusion of Ca in the electrode. It is noted that this invesitgation on Ca-Pb electrode sheds light on further research and design of electrode for Ca based liquid metal battery.

Keywords:

Liquid metal battery, molten salt electrolyte, Ca-Pb alloys, electrochemical properties.

1. Introduction

The liquid metal battery (LMB) has attracted more and more attention especially for its application for grid storage, it is considered as a promising electrochemical energy storage device because of its long cycle life, low-cost and easier scale-up. [1-2] Different from other battery systems, LMB has an unique three liquid layer structure which composed of a liquid anode, electrolyte and cathode. Due to the density differences and immiscibility, the cell can self-segregate into three distinct layers at the operating temperature. [3] The anode is on the top and cathode is on the bottom, both of which are electrically isolated by molten salt electrolyte. Attributed by the three liquid layers structure design of the liquid metal battery, the liquid-liquid electrode/electrolyte interface brings the facile charge transfer and fast mass transport between the liquid electrode and electrolyte. [4-6] Meanwile, the molten salt electrolyte has a high electrical conductivity and thus a low ohmic loss. [7-9] The combination of the above two features enables the LMB to be worked at high charge/discharge rates which is quite suitable for grid storage.

Till now, the development of the electrode system for LMB mainly focus on the Lithium based system, attributing to the lowest electronegativity and the lowest solubility of Lithium in its halide

salts. [10] Li||Bi [3], Li||Bi-Sb [11], Li||Sb-Pb [12], Li||Sb-Sn [13], Li||Te-Sn [14] and Li||Sb-Bi-Sn [10] were intensive investigated. The results show that the lithium based LMB deliver the average discharge voltage of 0.6-1.2 V and energy densities of 60-150 Wh kg^{-1}. However, considering the booming industry of Lithium ion battery, the restricted Lithium supply for LMB and the ripid price increasing of Lithium can not be ignored.

Calcium is the fifth abdount element in the earth's crust, which also shows the low standard reduction potential of −2.87 V vs NHE. These features make Ca as a sustainable negative electrode material of LMBs considering its application for large-scale energy storage. Several fundmental studies on the thermodynamic and electrochemical properties of calcium-based LMB systems have been reported, such as Ca||Sb [15-16] and Ca||Bi [17-18]. They show the competitive battery performance comparing with Lithiun based system. However, in view of the cost of antimony and bismuth, Ca-Pb electrode couple was considered to have the good voltage (~ 0.6 V) and the lowest cost (~36 \$ kWh^{-1}) among various optional materials for Ca based LMBs. [2] Meanwhile, Pb can also be as the alloy element to form Sb-Pb and Bi-Sb as the alloy positive electrode, which can also contribute to the capacity beyond Sb and Bi. However, Ca has high solubility in its halide salts [19], which lead to the high self-discharge current in the Ca based LMB and therefore the low coulombic efficiency. It is differcult to measure the electrochemical properties of Ca-Pb in molten salt electrolyte. Hence, Kim et al. investigated the thermodynamic properties of Ca-Pb alloy by using

CaF_2 solid electrolyte, which has proved its potential application in LMBs. [20]

Herein, in our works, we employed a multi-cation molten salt (LiCl-NaCl-$CaCl_2$) as the electrolyte to supress the solubility of Ca in molten salts. We proved the stability of the Ca-Pb system in a multi-cation electrolyte by measuring the electromotive force (*emf*) of the Ca-Pb electrode. Then, the electrochemical properties of Pb as the positive electrode for the potential application in LMBs and the alloying-dealloying processes of Ca with Pb electrode were investigated in details.

The alloying and dealloying processes of Ca with Pb at the interface between the electrolyte and Pb electrode are illustrated as follows: during the alloying processes, the Ca^{2+} cation conducts through the electrolyte (mass transport), then it is reduced and alloyed with Pb (charge transfer), and the Ca metal is diffused from the surface to the bulk of electrode (mass transport). The reverse processes occur when the electrode is dealloyed.

The electrochemical cell in our study can be represented by the following formula:

$$Ca|LiCl\text{-}NaCl\text{-}CaCl_2|Pb, \qquad (1)$$

where a multi-cation molten salt of LiCl-NaCl-$CaCl_2$ was served as the electrolyte with a mole fraction of 38.5-26.5-35.0 (T_m=457℃). The operating temperature was set at 600℃ and 700℃ according to the Ca-Pb binary phase diagram (Fig. 1). [21]

The potentials of the Ca-Pb electrode are calibrated to the value versus pure Ca(*s*) by the

following equation:

$$E = E_{WE} + E_{ref}, \qquad (2)$$

where E_{WE} is the potential of Ca-Pb working electrode versus Ca-Bi reference electrode, E_{ref} is the potential of the reference electrode versus pure Ca(s), and its values are 0.785 V at 600℃ and 0.765 V at 700℃ from the literature. [15]

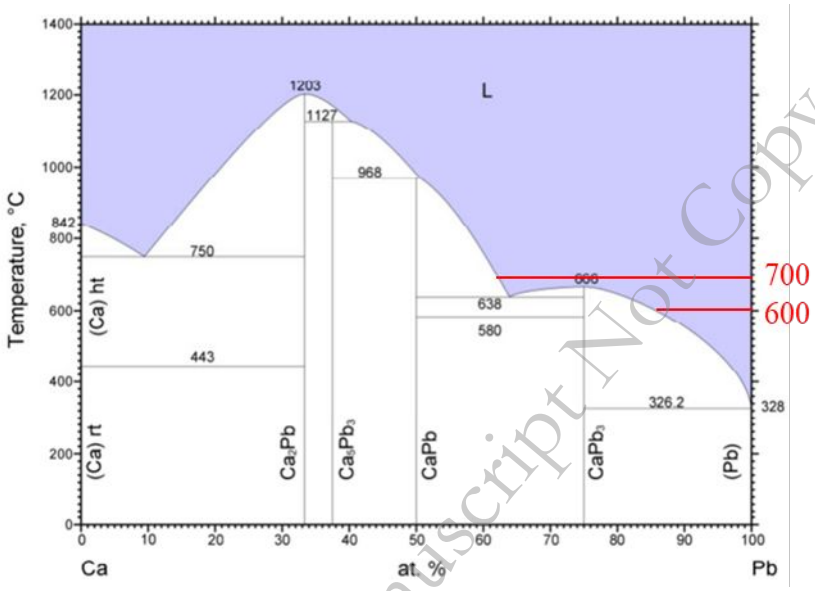

Fig. 1. The Ca-Pb binary phase diagram. [21]

2. Experimental

2.1 Materials preparation

The pure Pb (99.999%, Alfa Aesar) was pre-melted in a boron nitride (BN) crucible (Saint-Gobain Advanced Ceramics) inside the glovebox with an inert argon atmosphere (O_2 < 0.1 ppm, H_2O < 0.1 ppm), which was served as the working electrode (WE). A Ca-Bi alloy (x_{Ca} = 0.15) was as the counter electrode (CE) by melting pure Bi (99.999%, Alfa Aesar) and Ca (99.99%, Aldrich) also in a BN crucible. To provide facile transfer kinetics, it is necessary to ensure that the surface

area of CE is much larger than that of WE. A Ca-Bi alloy (x_{Ca} = 0.35) was adopted as the reference electrode (RE), which was prepared in the same way. It should be noted that in order to make sure the stability of the RE potential, the reference electrode of Ca-Bi alloy (x_{Ca} = 0.35) was a mixture of $Ca_{11}Bi_{10}$ (solid) and Bi (liquid), which is in the the two-phase region. Its potential is fixed and does not change with the composition. [22]

The high-purity anhydrous salts of LiCl (99.995%, Alfa Aesar), NaCl (99.99%, Alfa Aesar), and $CaCl_2$ (99.99%, Alfa Aesar) were used to prepared the 38.5-26.5-35.0 mol% LiCl-NaCl-$CaCl_2$ electrolyte. To obtain dry and homogenous electrolytes, the molten salt were pre-melted in the stainless crucible by following procedures: 1) placed the electrolyte in a heatable sealed container, evacuated it to a pressure below 1 Pa and heated it to 80℃, then maintained the vacuum and temperature for 12 hrs；2) increased its temperature from 80 to 250℃ and maintained the vacuum and temperature at 250℃ for 12 hrs; 3) heated the electrolyte to 700℃ and kept it for 3 hrs under the flowing argon gas; 4) The pre-melted electrolyte was grounded into lumps with 5-10 mm in diameters in the glove box after cooling down to room temperature.

2.2 Electrochemical cell assembly

The three-electrode electrochemical cell was assembled in a glove box as well. During the induction melting process, the tungsten wires with a diameter of 1 mm (99.95%, Alfa Aesar) were inserted into each electrode to establish electrical contact with the electrodes. The wire was wrapped

in an alumina tube (99.8%, McDanel Advanced Ceramic Technologies). The prepared three electrodes were arranged into an alumina crucible (99.8%, McDanel Advanced Ceramic Technologies). Then the electrolyte were added to cover the electrodes. The electrochemical cell was put in a stainless steel chamber. The configuration of the experiment is shown in Fig. 2.

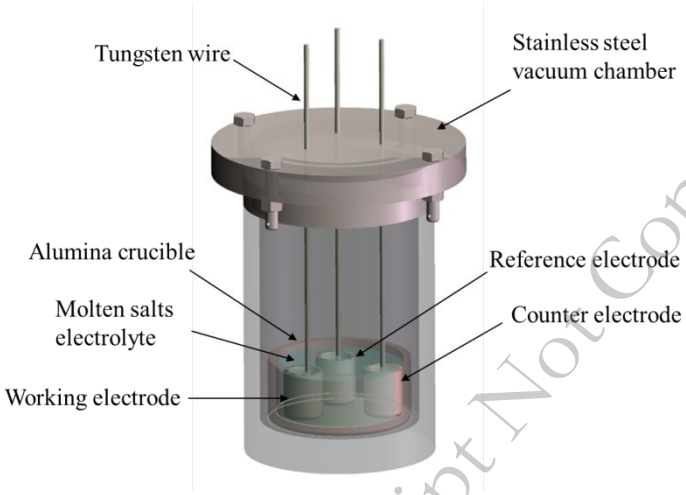

Fig. 1. Electrochemical cell configuration: three-electrode setup comprising the working electrode (WE), reference electrode (RE), and counter electrode (CE).

2.3 Electrochemical measurements

The electrochemical measurements were carried out by a potentiostat-galvanostat (PGSTAT302N) and a frequency response analyzer (FRA32M). During the coulometric titration experiment, the current density of 50 mA cm^{-2} was used. The dwelling time of the alloying and dealloying of Ca with Pb of each step was set as 3000 s, and the relaxation time of 5000 s was to obtain the accurate equilibrium electrode potential (E_{eq}) after each step. The estimation of the mole fraction of Ca in WE ($x_{Ca(inPb)}$) was on the assumption of 100% coulombic efficiency in this study. To assess the rate capability, the potential of the WE was recorded at different current density.

Finally, to obtain the self-discharge current of the cell, the electrode potential of WE was holding at 0.45 V and 1.40 V for 12 hrs at 600 ℃ and 700°C. Furthermore, electrochemical impedance spectroscopy (EIS) was performed using CHI electrochemical analyzer (CHI 660E) to accurately analyse the total resistance of WE, which was carried out at the open circuit potential with a perturbation amplitude of 5 mV and a frequency range of 10 kHz to 0.01Hz.

2.4 Post-mortem analysis

The working electrodes at different stages during the alloying process were quenched for post-mortem analysis. The electrodes were examined by a stereomicroscope (Olympus SZ61) to observe the macroscopic morphology, and then the microscopic morphology and composition were analyzed by using a scanning electron microscopy (SEM, JEOL6610) and an energy dispersive X-ray spectrometry (EDS, IXRF System, Model 55i).

3. Results and discussions

3.1 *emf* measurements of Ca-Pb alloy in the molten salt electrolyte

In order to measure the equilibrium potential of Ca-Pb working electrode in the LiCl-NaCl-$CaCl_2$ molten salt electrolyte exactly, the coulometric titration method was adopted. All measured results were compared with the data from the literature by using CaF_2 solid electrolyte to verify the reliability of the multi-cation molten salt electrolyte [20], because the CaF_2 has confirmed to have extremely low solubility of Ca metal in previous study [23].

The variation of the potential of Ca-Pb working electrode (E) and the current density (j) at 600°C is shown in Fig. 3a. It should be pointed out that the equilibrium potential values measured during the twelfth and thirteenth dealloying steps were removed due to the drastically change of the electrode potentials. The equilibrium potentials of Ca-Pb electrode at each mole fraction of Ca in the electrode were extracted from the value of the open circuit potential after each titration step. Fig. 3(b) (c) and Tab. 1 show the relationship of the equilibrium potentials of Ca-Pb electrode and the mole fraction of Ca in the electrode. The test was performed at two different temperatures because the depth of the titration varies with temperature, which can be seen from the Ca-Pb phase diagram in Fig. 2. By comparing the data from our study and the literature (shown in Fig. 3 and Tab. 1), we can conclude that the *emf* values measured by using the multi-cation molten salt as the electrolyte and that from CaF_2 solid electrolyte are generally in good agreement (the difference is less than 3%), which indicates the multi-cation molten salt electrolyte can effectively diminish the solution of Ca in the electrolyte. The slight differences may arise from the existence of self-discharge current. As shown in Fig. 3c, the *emf* values continue to drop to 0.5V and that tend to stabilize after decrease to 0.6V in Fig. 3b, which is caused by the increase in the solubility of Ca in Pb with increasing temperature.

(a)

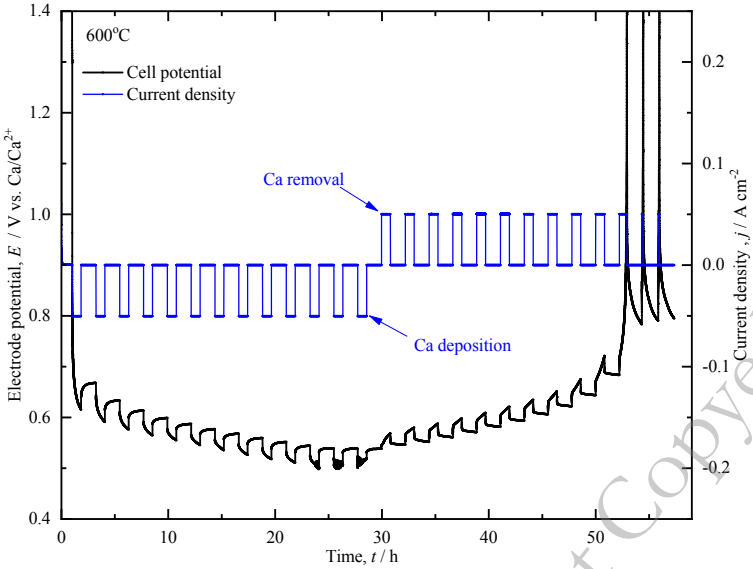

(b)

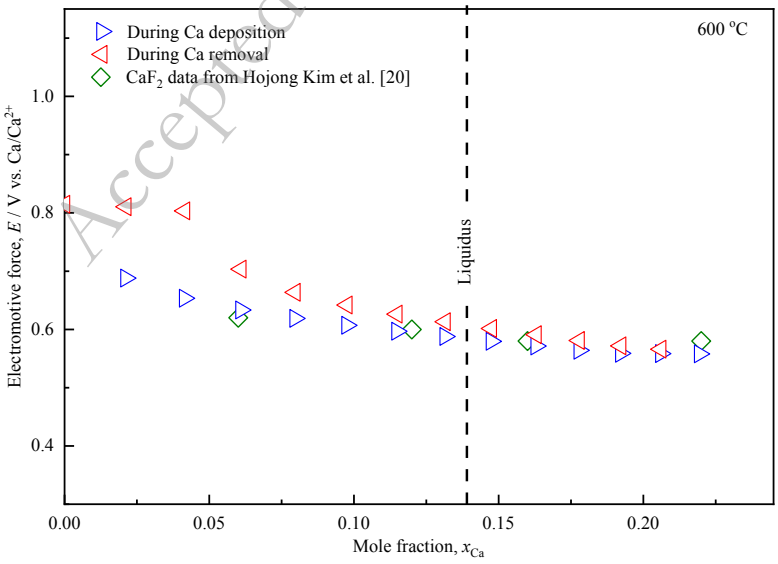

(c)

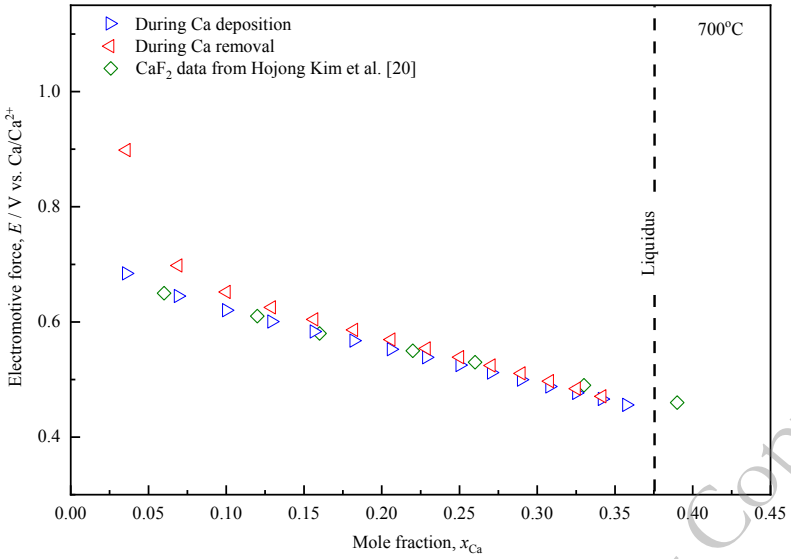

Fig. 3. (a) Potential of the WE and current density during the measurement in the coulometric titration at 600℃, (b) E_{eq} values of the WE as a function of composition of the Ca-Pb electrode at 600℃ and (c) 700℃.

Table 1. Equilibrium potentials of Ca-Pb alloys from coulometric titration (this work) and previously reported *emf* values obtained using CaF_2 [20]

	600℃		700℃	
x_{Ca}	This work	Ref. [20]	This work	Ref. [20]
0.02	0.69	-	-	-
0.04	0.65	-	0.68	-
0.06	0.63	0.62	-	0.65
0.07	0.62	-	0.65	-
0.10	0.61	-	0.62	-
0.11	0.60	-	-	-
0.12	-	0.60	-	0.61
0.13	0.59	-	0.60	-
0.15	0.58	-	-	-

0.16	**0.57**	**0.58**	**0.58**	**0.58**
0.18	**0.56**	**-**	**0.57**	**-**
0.19	**0.56**	**-**	**-**	**-**
0.21	**0.56**	**-**	**0.55**	**-**
0.22	**0.56**	**0.58**	**-**	**0.55**
0.23	**-**	**-**	**0.54**	**-**
0.25	**-**	**-**	**0.53**	**-**
0.26	**-**	**-**	**-**	**0.53**
0.27	**-**	**-**	**0.51**	**-**
0.29	**-**	**-**	**0.50**	**-**
0.31	**-**	**-**	**0.49**	**-**
0.33	**-**	**-**	**0.48**	**0.49**
0.34	**-**	**-**	**0.47**	**-**
0.35	**-**	**-**	**-**	**-**
0.36	**-**	**-**	**0.46**	**-**
0.39	**-**	**-**	**-**	**0.46**
0.42	**-**	**-**	**-**	**-**

3.2 Kinetics of Ca-Pb alloying and dealloying

To evaluate the kinetics of Ca-Pb alloying and dealloying process, the potential of Ca-Pb electrode was obtained at the current density range from 50 to 200 mA cm^{-2} at 600℃ and 700℃. The corresponding results are shown in Fig. 4. The cut-off voltage of the electrode was set as the value where the potential changes dramaticly in this test. From Fig. 4a and 4b, we can see that the electrodes exhibite highly chemically reversible electrode reaction. It is obviously that with the current density increasing, the overpotential of Ca-Pb electrode is also increased. And the lower discharge capacity was found at the higher current densities. The electrode potential always showed a sharp decrease near the end of Ca-Pb alloying process, which may result from the nucleation of

solid Ca-Pb intermetallic at the interface of liquid electrode/electrolyte.

(a)

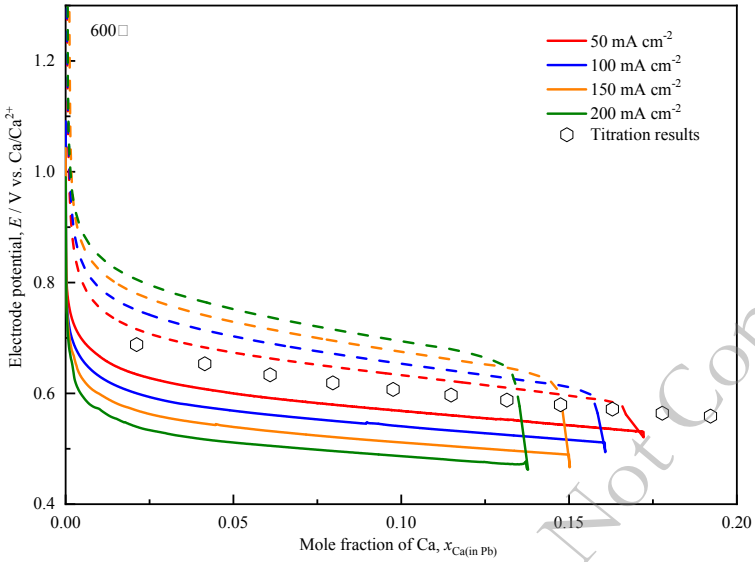

(b)

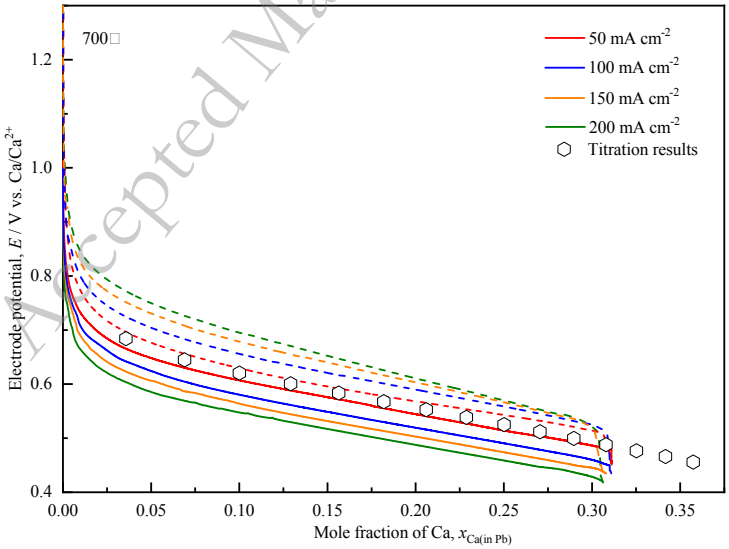

Fig. 4. The potential of the WE, *E*, measured as a function of current density during continuous alloying and dealloying of Ca with the Pb electrode and the E_{eq} values at (a) 600℃

and (b) 700℃.

3.3 The electrochemical performances of Ca-Pb alloy

Coulombic efficiency is vital important to evaluate the electrochemical properties for Ca||Pb cell. The coulombic efficiency of the Ca-Pb electrode at 600℃ is estimated on the base of the data from Fig. 4a and the corresponding results are shown in Tab. 2. It is clearly to see that the coulombic efficiency of the cell increased from 98.8% to 102.4% with the current density gradually increasing from 50 mA cm^{-2} to 200 mA cm^{-2}. The variation of coulombic efficiency at different current density can be attributed to the high self-discharge current of Ca-Pb electrode, which results from the high dissolution of Ca in the molten salt. Meanwhile, the dissolution of the Ca-Pb electrode in the electrolyte during alloying process will cause the loss of capacity, resulting in the phenomenon of exceeding 100% of coulombic efficiency in the following dealloying process.

Table 2. Coulombic efficiency at different current density at 600℃

Current density, j/mA cm^{-2}	Coulombic efficiency, η_c/%
50	98.84
100	99.27
150	100.0
200	102.42

To investigate the self-discharge current in Ca||Pb cell quantively, the electrode potential of WE was holding between 0.45 V and 1.40 V for 12 hrs. Fig. 5 shows the measured self-discharge current of Ca-Pb electrode at 600℃ and 700°C. It is easier to be found that the dealloying current flows when the electrode potentials are greater than 0.7 V. This may be caused by the chemical

transportant of Ca into Ca-Pb electrode; while when the electrode potential is less than 0.7V, the alloying current flows due to the Ca-Pb alloy dissolving in the electrolyte. [24] However, when the electrode potential is applied close to 0.7 V, the self-discharge current density decreases to zero. It was found that the self-discharging current for Ca-Pb is as low as 2 mA cm^{-2} at 600°C comparing with that at 700°C, which makes the cell have a high coulombic efficiency and ensures the accuracy of the electrode potential measurement. This phenomenon may also prove that the self-discharge current is mainly generated from the dissolution of Ca in the molten salt.

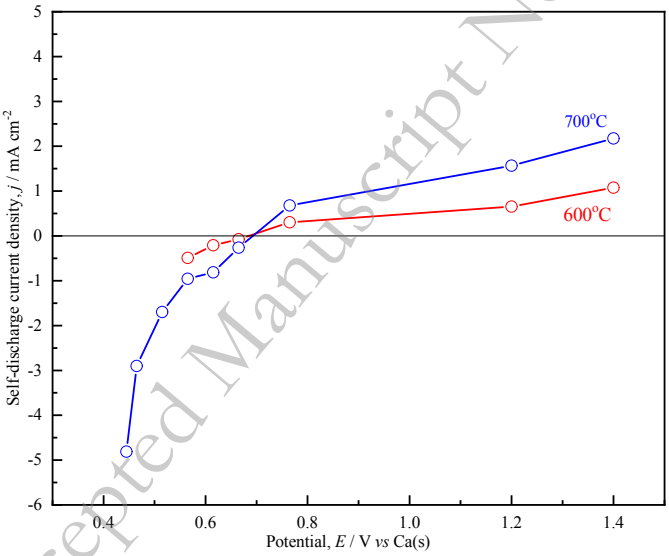

Fig. 5. Self-discharge current densities, j_s, at different electrode potentials at 600℃ and 700℃.

To further understand the influence of the charge transfer and the mass transport on the electrochemical performance , the electrochemical impedance spectra (EIS) measurement was performed. Fig. 6a shows Nyquist plots of Ca-Pb electrode at the open circuit potentials at 700℃.

A semi-circle in the high frequency and a straight line in the low frequency can be seen clearly in the spectra. The high-frequency semi-circle intercept represents the ohmic resistance R_{ohm} and the semi-circle width represents the charge transfer resistance R_{ct}. The corresponding calculated impedance data of the charge transfer resistance, ohmic resistance and mass transfer resistance are tabulated in Tab. 3.

(a)

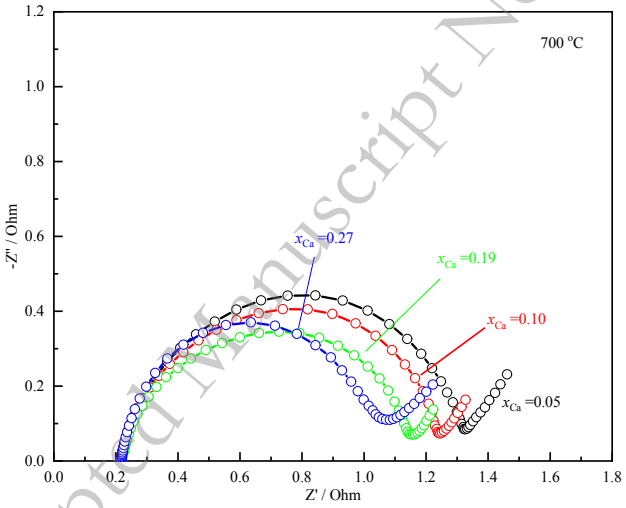

(b)

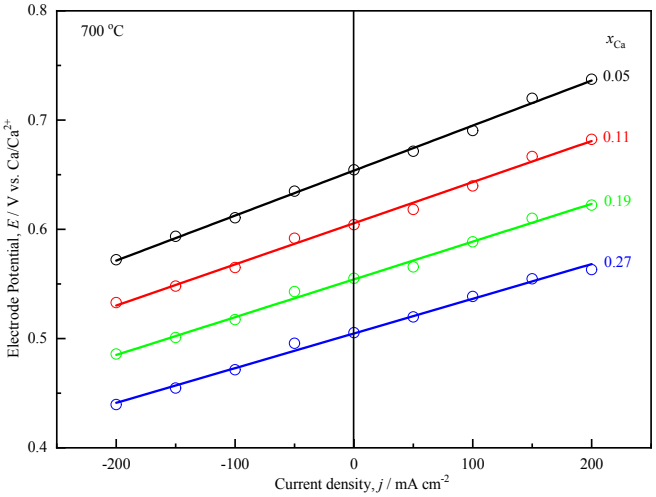

Fig. 6. (a) EIS was obtained at the open circuit potentials at 700℃, (b) The potential of WE as a function of current density at 700℃.

In the typical three-electrode setup of our work, the ohmic resistance R_{ohm} is only 0.06 Ω which show independent on the mole fraction of Ca, $x_{Ca(in\ Pb)}$. However, the charge transfer resistance R_{ct} is decreasing substantially with the increase of Ca concentration, from 0.30 Ω to 0.22 Ω. This may be attribute to the formation of uniformly Ca-Pb intermetallic compounds with the increasing of Ca concentration in the WE. Therefore the thickness of the liquid Pb is decreased in the electrode, which results in the reducing of the diffusion distance of Ca to Ca-Pb electrode and thus facilitated the alloying process. The mass transport resistance R_{mt} can be easy calculated by subtracting R_{ohm} and R_{ct} from the total resistance R_{tot}. The total resistance R_{tot} was acquired based on the calculation of the slope of the line in Fig. 6b. The corresponding results are also shown in Tab. 3. It is easy to see that the mass transport resistance R_{mt} only has a little contribution to the total resistance. From the above, it can be concluded that the charge transfer resistance R_{ct} plays a prominent role in the

electrochemical process of Ca-Pb alloying process.

Table 3. The EIS data of Ca-Pb electrode at 700°C

$x_{Ca(in\ Pb)}$	R_{tot} /Ω	R_{ohm} /Ω	R_{ct} /Ω	R_{mt} /Ω	j_0 /A
0.05	0.41	0.06	0.30	0.05	0.14
0.11	0.38	0.06	0.28	0.04	0.15
0.19	0.35	0.06	0.26	0.03	0.16
0.27	0.32	0.06	0.22	0.04	0.19

3.4 Post-mortem analysis

To investigate the microstructure evolution during the alloy process of Ca-Pb electrode, post-mortem analysis was carried out. Three different samples with different mole fraction of Ca were quenched to room temperature. All these Ca-Pb electrodes were prepared at 700℃ with 200 mA cm^{-2}. The mole fraction of Ca, $x_{Ca(in\ Pb)}$, of these three electrodes are 0.05, 0.15 and 0.31, respectively. The morphology of the electrodes and its composition are shown in Fig. 7. As shown in Fig. 7a, the concentration of Ca in WE was very low in the initially state during the alloying. The electrode was mainly composed of Pb and only a small amount of $CaPb_3$ can be found. As the content of Ca rised to $x_{Ca(in\ Pb)} = 0.15$, it can be found that the content of $CaPb_3$ increased in the two phase region in Fig. 7b.

When the electrode was in a composition where the potential dropped sharply, $x_{Ca(in\ Pb)} = 0.31$, it was observed that a large amount of $CaPb_3$ was generated in the electrode and a high-calcium

intermetallic CaPb appeared at the top of the electrode in Fig. 7c. The nucleation of CaPb may be due to the highly concentrated region of Ca formed when the electrode passing a high current. The formation of these solid intermetallics greatly reduces the activity of Ca, resulting in a sudden decrease in electrode potential. In particular, it was found these intermetallics $CaPb_3$ and CaPb did not accumulate at the interface between the electrode and the electrolyte but were uniformly distributed in the electrode. This indicates that the nucleation of solid intermetallics in the electrode will not hinder the diffusion of Ca in the electrode and will not cause a large loss of the coulombic capacity of the battery, which is consistent with the results in Fig. 4b.

(a)

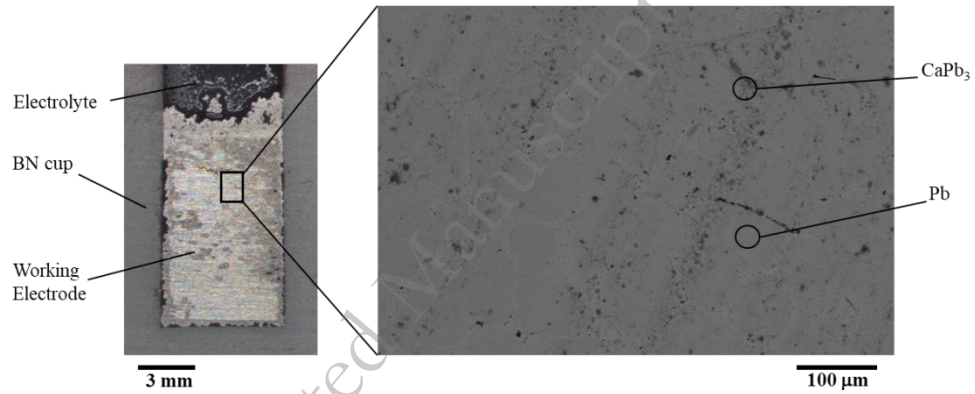

(b)

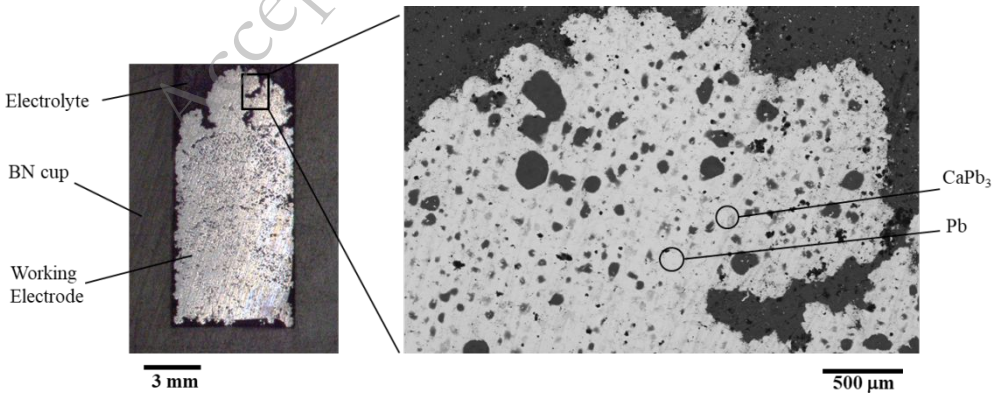

(c)

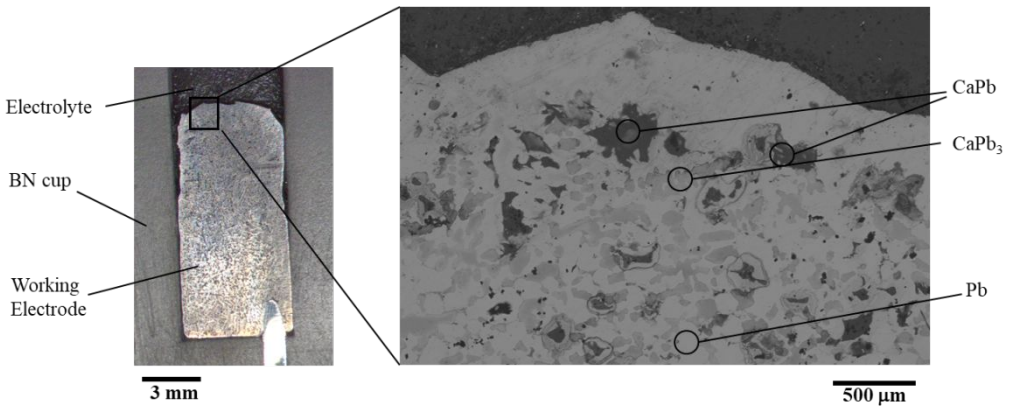

Fig. 7. Post-mortem analysis of the WEs with different mole fraction of Ca at a current density of 200 mA cm^{-2} at 700℃, (a) $x_{Ca(in\ Pb)}$ = 0.05, (b) $x_{Ca(in\ Pb)}$ = 0.15, (c) $x_{Ca(in\ Pb)}$ = 0.31.

4. Conclusions

The electrochemical properties of Ca-Pb as the positive electrode for LMB were evaluated in LiCl-NaCl-$CaCl_2$ molten salt. The solubility of Ca in electrolyte was successfully suppressed by using the alloy electrode and a multi-cation electrolyte. The electrode potential of Ca-Pb alloy and current density maintained a good linear relationship in the current density range from 50 to 200 mA cm^{-2}, it confirms that the Ca-Pb electrode has excellent kinetics performance. The Ca-Pb positive electrode exhibits a high discharge voltage of 0.6 V, and a high coulombic efficiency of 99%. Meanwhile, the cell has a small self-discharge current density. Near the end of Ca-Pb alloying process, a large amount of dispersed intermetallic $CaPb_3$ was found in the Ca-Pb electrode, which may result in a sudden drop in the electrode potential.

Acknowledgements

The authors would like to acknowledge the finanicial support from National Key R&D

Program of China (2018YFB0905600), National Natural Science Foundation of China (51874228, U1766216) and Natural Science Foundation of Shaanxi Province, China (2020JM-068).

References

[1] D. J. Bradwell, H. Kim, A. H. C. Sirk, and D. R. Sadoway, Magnesium–antimony liquid metal battery for stationary energy storage, *J. Am. Chem. Soc.*, 134(2012), p. 1895.

[2] H. Kim, D.A. Boysen, J.M. Newhouse, B.L. Spatocco, B. Chung, P.J. Burke, D.J. Bradwell, J. Kai, A.A. Tomaszowska, K.L. Wang, W.F. Wei, L.A. Ortiz, S.A. Barriga, S.M. Poize-au, and D.R. Sadoway, Liquid metal batteries: past, present, and future, *Chem. Rev.*, 113(2013), p. 2075-2099.

[3] X.H. Ning , S. Phadke, B. Chung, H. Yin, P. Burke, and D.R. Sadoway, Self-healing Li-Bi liquid metal battery for grid-scale energy storage, *J. Power Sources*, 275(2015), p. 370-376.

[4] H. A. Laitinen, R. P. Tischer, and D. K. Roe, Exchange current measurements in KCl‐LiCl eutectic melt, *J. Electrochem. Soc.*, 107(1960), No. 6, p. 546.

[5] A.D. Pasternak and D.R. Olander, Diffusion in liquid metals, *AIChE. J.*, 13(1967), No. 6, p. 1052.

[6] G. J. Janz and N. P. Bansal, Molten salts data: diffusion coefficients in single and multi-component salt systems, *J. Phys. Chem. Ref. Data*, 11(1982), No. 6, p. 505.

[7] L. Kartal and S. Timur, Direct electrochmical reduction of copper sulfide in molten borax, *Int. J. Miner . Metall. Mater.*, 26(2019), No. 8, p. 992.

[8] S.Q. Jiao and H. Zhu, Novel metallurgical process for titanium production, *J. Mater. Res.*, 21(2006), No. 9, p. 2172.

[9] T. Dai, L. Yang, X.H. Ning, D. Zhang, R. L. Narayan, J. Li, and Z.W. Shan, A low-cost intermediate temperature Fe/Graphite battery for grid-scale energy storage, *Energy Storage Mater.*, 25(2020), p. 801-810.

[10] W. Zhao, P. Li, Z.W. Liu, D.L. He, K. Han, H.L. Zhao, and X.H. Qu, High-performance antimony−bismuth−tin positive electrode for liquid metal battery, *Chem. Mater.*, 30(2018), p. 8739-8746.

[11] T. Dai, Y. Zhao, X.H. Ning, D.L. Zhang, R. L. Narayan, J. Li, and Z.W. Shan, Capacity extended bismuth-antimony cathode for high-performance liquid metal battery, *J. Power Sources*, 381(2018), p. 38-45.

[12] K.L. Wang, K. Jiang, B. Chung, T. Ouchi, P.J. Burke, D.A. Boysen, D.J. Bradwell, H.J. Kim, U. Muecke and D.R. Sadoway, Lithium antimony-lead liquid metal battery for grid-level energy storage, *Nature*, 514(2014), p. 348-350.

[13] H.M. Li, K.L. Wang, S.J. Cheng and K. Jiang, High performance liquid metal battery with environmentally friendly antimony-tin positive electrode. *ACS Appl. Mater. Interfaces*,

8(2016), p. 12830-12835.

[14] H.M. Li, K.L. Wang, H. Zhou, X.L. Guo, S.J. Cheng and K. Jiang, Tellurium-tin based electrodes enabling liquid metal batteries for high specific energy storage applications, *Energy Storage Mater.*, 14(2018), p. 267-271.

[15] S. Poizeau, H.J. Kim, J. M. Newhouse, B. L. Spatocco and D.R. Sadoway, Determination and modeling of the thermodynamic properties of liquid calcium–antimony alloys, *Electrochim. Acta*, 76(2012), 8–15.

[16] T. Ouchi, H.J. Kim, X.H. Ning, and D. R. Sadoway, Calcium-Antimony Alloys as Electrodes for Liquid Metal Batteries, *J. Electrochem. Soc.*, 161(2014), No.12, p. A1898-A1904.

[17] H.J. Kim, D.A. Boysen, D.J. Bradwell, B. Chung, K. Jiang, A.A. Tomaszowska, K. Wang, W. Wei, and D.R. Sadoway, Thermodynamic properties of calcium-bismuth alloys determined by emf measurements, *Electrochim. Acta*, 60(2012), p. 154.

[18] H.J. Kim, D. A. Boysen, T. Ouchi, and D.R. Sadoway, Calcium-bismuth electrodes for large-scale energy storage (liquid metal batteries), *J. Power Sources*, 241(2013), p. 239.

[19] R. A. Sharma, The solubilities of calcium in liquid calcium chloride in equilibrium with calcium-copper alloys, *J. Phys. Chem.*, 74(1970), No. 22, p. 3896.

[20] N.D. Smith, N.E. Orabona, J.P. S. Palma, Y.Kong, C. Blanchard and H.J. Kim, Thermodynamic properties of Ca-Pb electrodes determined by electromotive force

measurements, *J. Power Sources*, 451(2020), p. 227745.

[21] M. Idbenalia, C. Servantb, N. Selhaouia and L. Bouirdena, A thermodynamic reassessment of the Ca-Pb system, *CALPHAD: Comput. Coupling Phase Diagrams Thermochem.*, 32(2008), p. 64-73.

[22] C.J. Wen, B.A. Boukamp, R.A. Huggins, and W. Weppner, Thermodynamic and mass tra-nsport properties of "LiAl", *J. Electrochem. Soc.*, 126(1979), No.12, p. 2258.

[23] A.S. Dworkin, H.R. Bronstein, and M.A. Bredig, The electrical conductivity of solutions of metals in their molten halides. VIII. Alkaline Earth Metal Systems, *J. Phys. Chem.*, 70(1966), No.6, p. 2384.

[24] M. Okada, R. A. Guidotti, and J. D. Corbett, Solution of sodium alloys of some post-tra-nsition metals in molten sodium halides. Evidence for anions of bismuth and antimony, *I-norg. Chem.*, 7(1968), No.10, p. 2118.